

# Transient Current Distribution and Force Analysis of Three Phase Enclosure Type GIB Based on Field-Circuit Coupling FEM Method

Xiangyu Guan *ACES Member*, Bing Kang, Naiqiu Shu, Qiangqiang Yan, and Zipin Li

Department of Electrical Engineering  
Wuhan University, Wuhan, 430072, China  
Lzpwu@163.com

**Abstract** — On the purpose of optimal design and online monitoring of three phase enclosure gas insulated bus (GIB), a 3-D circuit-field coupling FEM model has been developed. The current constriction effects in plug-in connectors are simulated by modeling contact bridges between contact surfaces and the influence of conductor gravity on contact resistance has been taken into account. The distributions of current which is constrained by external circuit are obtained from field-circuit coupling calculation and electromagnetic force, which is derived from electromagnetic field calculation, is used as load inputs in mechanical field analysis. The validity of calculation model is demonstrated by comparing with vibration experiments. The dynamic current distribution and electromagnetic force behaviors of three phase enclosure GIB under steady state and different short circuit conditions have been analyzed using the calculation model. Analysis results show that the uneven heating of contact fingers due to current distributions under steady state and contact fingers with smaller contact forces are seriously ablated by large short currents under short circuit conditions, and are the main contact degradation mechanism of plug-in connector. Conductor electromagnetic forces under single phase short circuit condition are larger than those of two phase and three phase short circuit conditions and the electromagnetic force peak moments under different fault conditions are not the same.

**Index Terms** — Current distribution, electromagnetic force, field-circuit coupling, finite element method (FEM), GIB, plug-in connector, short circuit.

## I. INTRODUCTION

The three-phase enclosure type gas insulate bus (GIB) with the compact design by sealing the three phase conductors in a single metal tank filled with SF<sub>6</sub> gas has the advantages of land saving and high reliability [1]. During equipment operation, eddy currents in tank are induced by the alternating electromagnetic field which is induced by the conductor currents, and uneven electromagnetic forces are produced by the

interaction between current carriers and alternating electromagnetic field. The current distributions will cause uneven heating sources especially on plug-in connectors due to the existence of contact resistance and overheating fault may happen [2]. The electromagnetic forces can cause mechanical vibration of conductors and tank, and the contact force of connectors will decrease because of the existence of electromagnetic repulsion force between contact surfaces. Inadequate short-circuit strength may lead to a mechanical collapse of connectors and a damage of insulators when the large short circuit current flows through the device. So current distributions and electromagnetic force of GIB under normal and short circuit currents are key problems in equipment design and maintenance [3].

The image current method [4] is used to calculate the short circuit electromagnetic force in three phase enclosure type GIB [5], and the vibration of GIB is analyzed by assuming metal tank as thin cylindrical shell and the conductors as a transverse beam [6-7]. These methods are easy to formulate and fast to solve, however, the distributions of current and electromagnetic force of GIB are not uniform due to skin effect and proximity effect; these complex field patterns cannot be captured by using lumped parameter models, and numerical modeling techniques are established to represent these important phenomena occurring inside GIB [8-10]. There are two following main deficiencies existing in current numerical models of GIB. First, plug-in connectors are not included so the electro repulsion force [11-12] and current distributions in plug-in connector cannot be considered. Second, nonlinear transient current and electromagnetic field of GIB are constrained by external circuit, thus belonging to the typical field-circuit coupling problem [13-17].

The time-varying electromagnetic force of three phase enclosure GIS based on contact bridge model has been introduced in our previous work [18]. Focus on the current and force distributions in GIB under normal and short circuit conditions, a 3-D field-circuit coupling FEM model of three phase enclosure type GIB is developed. The structure of the GIB is shown in Fig. 1.

Three phase conductors are fixed with disc-type insulators, the plug-in connectors containing 16 contact fingers arranged clockwise around the center conductor axis are used to eliminate the influence of thermal stress on insulators. An acceleration sensor (A1) placed on tank is used to measure the vibration of tank. Assumptions about the calculation model are as follows:

- The working current frequency is 50 Hz, so the electromagnetic field calculation model is based on the quasi-static approximation.
- The variation in electric field cannot influence magnetic field. To be clear, some parts chamfers which are used to improve electric field have been neglected for the simplicity of calculation.
- The influence of conductor and tank deformation on the electromagnetic field distribution is neglected.
- Though there is a difference between mechanical and electrical contact area, only mechanical contact area is considered for the chemical stability of SF<sub>6</sub> gas.
- The springs of connector are neglected.
- The nonlinearity of the material and the displacement current are neglected.

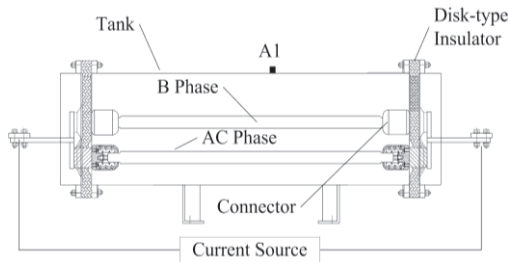


Fig. 1. Schematic structure of three phase enclosure type GIB.

## II. ANALYSIS METHOD

### A. Solution regions and boundary conditions

The solution region and boundary conditions of the field-circuit coupling model are shown in Fig. 2. The solution region contains circuit region which is excited by three-phase voltage source, and FEM region which is connected with extern circuit by coupling node voltage sources. The tank surrounded by air is filled with SF<sub>6</sub> gas and the eddy currents which are induced by the time-varying conductor currents flowing through it.

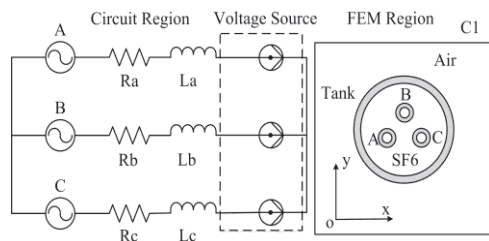


Fig. 2. Solution regions and boundary conditions.

### B. Contact bridge model

The contact resistance and the electromagnetic repulsion force exist between bus connectors and contact fingers due to current constriction effect in the contact interface. A contact bridge model which takes into account the influence of conductor gravity has been developed (Fig. 3). The height of contact bridge is 0.2 mm and the radius of contact bridge can be calculated as the Hertz formula [19]:

$$a = (3F_j R^* / 4E^*)^{1/3}, \quad (1)$$

where  $a$  is the contact bridge radius,  $F_j$  is the contact force of one contact finger which is influenced by the spring holding force and the normal component of conductor gravity.

The equivalent contact radius  $R^*$  is illustrated in Fig. 3, and the equivalent Young's modulus  $E^*$  of plug-in connector can be described as:

$$1/E^* = [(1-\nu_1^2)/E_1 + (1-\nu_2^2)/E_2], \quad (2)$$

where  $E_1$ ,  $E_2$  are Young's modulus of conductor and contact finger,  $\nu_1$ ,  $\nu_2$  are Poisson's ratio of conductor and contact finger. All these parameters can be obtained from special GIS bus bar capsule design.

The one finger contact force of plug-in connector exerted by three circular holding springs and the normal component of conductor gravity can be calculated as:

$$F_j = 3K\pi^2(D_1 - D_0)/n - G_n, \quad (3)$$

where  $K$  is the spring stiffness coefficient,  $\pi$  is the circular constant,  $n$  is the number of fingers and  $n=16$ ,  $D_0$  and  $D_1$  are the diameters of the spring center line before and after loading respectively.  $G_n$  is the normal component of conductor gravity exerting on one contact finger.

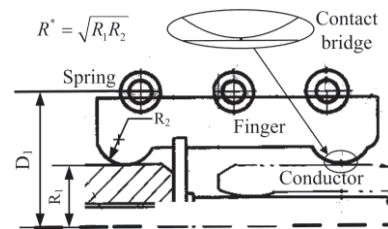


Fig. 3. Contact bridge between plug-in connector and conductor.

### C. Calculation method

The flow chart for solving the coupled fields of GIB is shown in Fig. 4. The electromagnetic field of GIB and extern circuit are connected to each other by the coupling node voltage sources. A sequentially coupling method is used to simulate the interactions between electromagnetic and mechanical fields. The initial conditions such as contact forces and contact bridge radiuses are calculated from single mechanical analysis without load currents. New contact force can be obtained from mechanical field analysis which uses

nodal electromagnetic forces as load inputs and the contact radius should be changed. Such process is conducted until the contact radius converged.

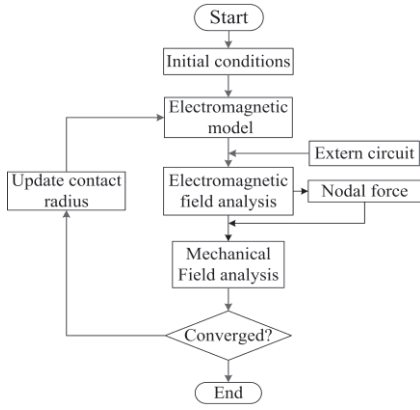


Fig. 4. Flow chart of field-circuit coupling calculation process.

### III. FIELD-CIRCUIT COUPLING ANALYSIS

#### A. Electromagnetic field analysis

The quasi-static approximation can be used since steady state AC flows in the bus conductor.

With the magnetic vector potential  $\mathbf{A}$ , the Maxwell's equations can be rewritten as:

$$\left. \begin{aligned} \nabla \times \mathbf{H} &= \mathbf{J} \\ \nabla \times \mathbf{E} &= -\frac{\partial \mathbf{B}}{\partial t} \\ \mathbf{B} &= \nabla \times \mathbf{A} \end{aligned} \right\} \quad (4)$$

The governing equation of electromagnetic field (4) can be derived as:

$$\nabla \times \mu(\nabla \times \mathbf{A}) = \mathbf{J}, \quad (5)$$

where  $\mu$  is magnetic permeability.

The governing Equation (5) can be rewritten as the form of Poisson's Equation (8) by using the vector Equation (6) and the Coulomb's gauge (7):

$$\nabla \times (\nabla \times \mathbf{A}) = \nabla(\nabla \cdot \mathbf{A}) - \nabla^2 \mathbf{A}, \quad (6)$$

$$\nabla \cdot \mathbf{A} = 0, \quad (7)$$

$$\nabla^2 \mathbf{A} = -\mu \mathbf{J}, \quad (8)$$

where the total current  $\mathbf{J}$  consists of the source current  $\mathbf{J}_s$  and the eddy current  $\mathbf{J}_e$ , that is:

$$\mathbf{J} = \mathbf{J}_s + \mathbf{J}_e. \quad (9)$$

The voltage drop of conductor (coupling node voltage source) which is the key to combining the extern circuit with FEM model can be calculated:

$$V_{drop} = \int_V c_i \left(-\frac{\partial \mathbf{A}}{\partial t}\right) dV, \quad (10)$$

where  $V$  is the conductor volume,  $c_i$  is the loop coefficient,  $c_i=1$  if conductor inside loop  $i$ , otherwise  $c_i=0$ .

The eddy current in the conducting material is:

$$\mathbf{J}_e = \sigma \mathbf{E} = -\sigma \frac{\partial \mathbf{A}}{\partial t}, \quad (11)$$

where  $\sigma$  is electrical conductivity.

The boundary conditions of electromagnetic field are as follows:

$$\mathbf{A}|_{C_1} = 0, \quad (12)$$

$$\left. \begin{aligned} \mathbf{A}_1 &= \mathbf{A}_2 \\ \mu_1 \nabla \times \mathbf{A}_1 \cdot \mathbf{n}_{12} &= \mu_2 \nabla \times \mathbf{A}_2 \cdot \mathbf{n}_{12} \\ n \cdot (-j\omega \varepsilon \mathbf{A} - \varepsilon \nabla \phi) &= 0 \end{aligned} \right\} \text{ in } S, \quad (13)$$

where  $C_1$  is the boundary of FEM region,  $S$  is the boundary of conductor material and no current regions (gas),  $\varepsilon$  is dielectric constant of conductor material.

#### B. Extern circuit analysis

According to the Kirchoff's voltage law (KVL), the extern circuit equation can be expressed as:

$$U = RI + L \frac{dI}{dt} + G \frac{d\mathbf{A}}{dt}, \quad (14)$$

where  $R$  is the total resistance which consists of line resistance and load resistance,  $L$  is the total inductance,  $G$  is a matrix which depends on the geometrical features of the GIB.  $I$  is the node current matrix,  $\mathbf{A}$  is the node magnetic vector matrix,  $U$  is the external voltage matrix. Three-phase voltage under symmetric power frequency can be represented as follows:

$$\left. \begin{aligned} u_A &= \sqrt{2}U \cos(\omega t + 0^\circ) \\ u_B &= \sqrt{2}U \cos(\omega t - 120^\circ) \\ u_C &= \sqrt{2}U \cos(\omega t + 120^\circ) \end{aligned} \right\} \quad (15)$$

#### C. Electromagnetic field-circuit coupling analysis

The global field-circuit coupling equations can be written as:

$$\begin{bmatrix} 0 & 0 \\ G & L \end{bmatrix} \frac{\partial}{\partial t} \begin{Bmatrix} \mathbf{A} \\ \mathbf{I} \end{Bmatrix} + \begin{bmatrix} K_e & D \\ 0 & R \end{bmatrix} \begin{Bmatrix} \mathbf{A} \\ \mathbf{I} \end{Bmatrix} = \begin{Bmatrix} 0 \\ U \end{Bmatrix}, \quad (16)$$

where  $K_e$  is the stiffness matrix of magnetic vector potential,  $D$  is the loading matrix.  $K_e$  and  $D$  can be obtained by the finite element analysis.

A backward time stepping scheme is used for the time discretization and the minimum time step is set to 0.3ms in order to simulate the transient process of alternating electromagnetic field:

$$\left\{ \frac{\partial \mathbf{A}}{\partial t} \right\}^{t+\Delta t} = \frac{\mathbf{A}^{t+\Delta t} - \mathbf{A}^t}{\Delta t}, \quad (17)$$

$$\left\{ \frac{\partial \mathbf{I}}{\partial t} \right\}^{t+\Delta t} = \frac{\mathbf{I}^{t+\Delta t} - \mathbf{I}^t}{\Delta t}. \quad (18)$$

#### D. Electromagnetic forces

The electromagnetic forces of three phase enclosure type GIB which induced by the interaction between

current carriers and alternating magnetic field caused by current carriers can be expressed as:

$$\mathbf{F} = \int_V \mathbf{J} \times \mathbf{B} dV. \quad (19)$$

#### IV. MECHANICAL ANALYSIS

The mechanical vibration of three phase enclosed type GIB during operation can be induced by the altering electromagnetic force. The mechanical governing equation coupled with electromagnetic force can be written as:

$$[M][\ddot{\mathbf{u}}] + [K][\mathbf{u}] = [\mathbf{F}_e], \quad (20)$$

where  $M$  is the mass matrix,  $K$  is the stiffness matrix,  $\mathbf{u}$  is the nodal displacement vector matrix and  $\ddot{\mathbf{u}}$  is the nodal acceleration vector matrix.  $\mathbf{F}_e$  is the nodal force vector matrix which includes electromagnetic force and conductor gravity.

The boundary conditions of mechanical field can be expressed as follows.

Conductors are supported by the two ending plug-in connectors and the aluminum alloy tank is fixed on the ground through the bracket.

In order to resist the impact of short circuit current, plug-in connectors of GIB have positioning design which allows the contact fingers referring only to radial freedom (direction of contact force) and without axial freedom.

#### V. CALCULATION MODEL

A 3-D FEM model of three phase enclosure GIB has been developed for the multi-physics calculation. The material and geometrical properties are shown in Table 1. The line inductance (67 mH) and the line resistance (1.5  $\Omega$ ) which get from one 220 kV gas insulated substation in China Southern Power Grid Company.

16 pieces of contact fingers are arranged clockwise in the xoy coordinate plane, and the gravity acceleration is along the  $-y$  direction. Using the mechanical analysis, the initial contact forces between each contact spot deriving from the contact spring and the gravity of conductors are shown in Fig. 5 (a), and the contact bridge radiuses of each contact fingers can also be calculated (Fig. 5 (b)), which indicates that the contact forces and the contact radiuses increase from upper contact fingers to lower ones for the action of conductor gravity.

Table 1: Simulation model parameters

Tank Material	Aluminum alloy 6063-T6
Finger Material	Copper T2Y
Finger Number	16
Shield Material	Aluminum alloy 6063-T6
Bus Material	Aluminum alloy 6063-T6
Insulator Material	Epoxy resin
Tank Size	$\Phi 596/\Phi 580$
Bus Size	$\Phi 90/\Phi 60$
Span	2300 mm

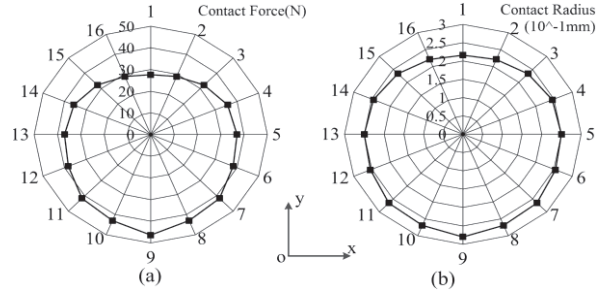


Fig. 5. Initial conditions of contact force and contact bridge radius versus contact fingers: (a) contact force, and (b) contact bridge radius.

#### VI. STEADY-STATE FIELD ANALYSIS

Using the field-circuit coupling FEM calculation model, the current density, electromagnetic force and tank vibration characters under steady-state are calculated. The validity of calculation model is demonstrated by vibration experiments.

##### A. Field distributions

The current density distributions of conductors and tank at  $t=5$ ms (peak time of A phase current) under normal load current (1000A) are shown in Fig. 6 (a). It can be seen from current distribution results that the current densities in conductors and tank are not uniform due to proximity effect and eddy effect. Current distributions of different contact fingers are strongly influenced by the interactions between different phase conductor currents (Fig. 6 (b) and Fig. 6 (c)). From calculation results we can deduce one contact failure mechanism of three phase enclosure type GIB under steady state is that the contact finger fevers vary each other due to the uneven current distributions between different contact fingers; some contact fingers where larger currents flow through may cause overheating and failure first, other contact fingers then overheating due to the load current increasing with fewer contact fingers and eventually caused the whole connector failure.

The nodal electromagnetic forces of conductors and tank at  $t=5$ ms (peak time of A phase current) under normal load current (1000A) are shown in Fig. 6 (d). Distributions of electromagnetic forces in conductors and tank are influenced by the distributions of currents and the nodal electromagnetic forces of A phase conductor and corresponding tank part are larger than other parts of GIB. The distributions of electromagnetic forces in different contact fingers are similar to current distributions (Fig. 6 (e) and Fig. 6 (f)) and the electromagnetic force of individual contact finger under normal load current is rather small compared with contact force (about 37N). So the main factor affecting the stability of GIB connector under normal operation conditions refers to the uneven heating of contact fingers rather than the action of electromagnetic force.

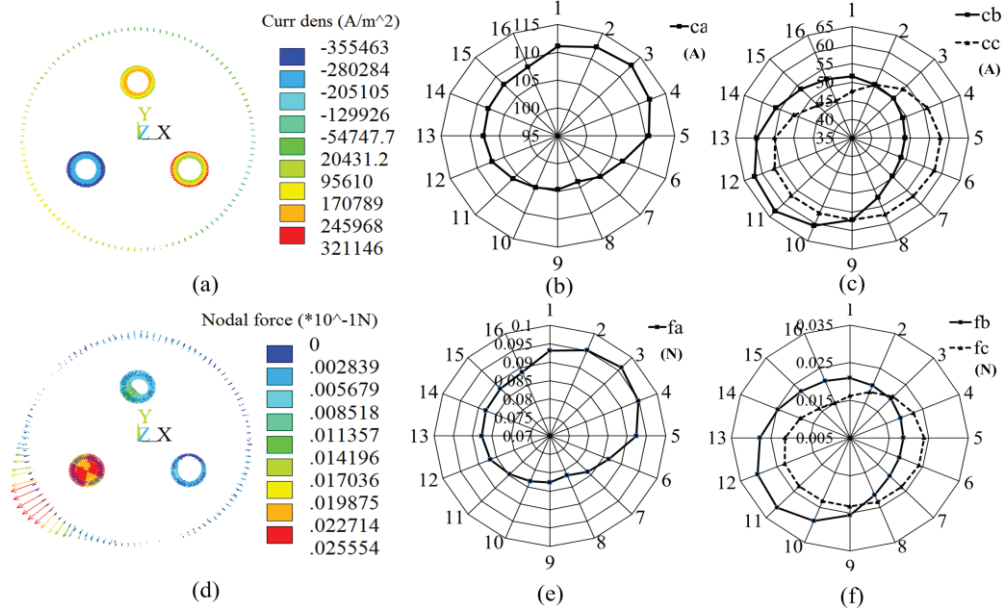


Fig. 6. Electromagnetic field distribution at  $t=5\text{ms}$ : (a) current density distributions, (b,c) absolute values of contact finger currents, (d) electromagnetic force distributions, and (e,f) contact finger electromagnetic forces.

**B. Tank vibration under normal operation**

In order to qualitatively validate the numerical results, vibration tests have been performed on a three phase enclosure type GIB capsule (Fig. 1). Tank vibration results obtained from calculation model and vibration test under AC steady state (1000A) show good agreement in Fig. 7. It can be seen from the results that vibration of tank under AC steady state mainly consists of electromagnetic vibration with 2 times of power frequency and the vibration amplitude is small (0.2 mm).

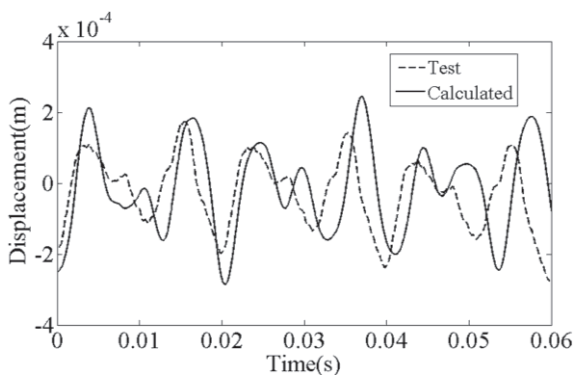


Fig. 7. Time varying curve of tank vibration under AC steady state.

**VII. ELECTROMAGNETIC FORCE UNDER SHORT CIRCUIT CONDITIONS**

The three phase enclosure type GIB will carry full short-circuit currents of the power system since it is a

series device. Larger power losses and electromagnetic forces may be induced by considerable short circuit currents. The short electromagnetic forces under different short circuit conditions are essential for analyzing the short circuit withstand capability of GIB. The line resistance and line inductance of external circuit are used to simulate the short circuit fault and the distributions of electromagnetic force are computed at the first peak of the B phase short-circuit current (6.7ms).

**A. Distributions of short circuit electromagnetic force of conductors and tank**

The electromagnetic force distributions of conductors and tank at  $t=6.7\text{ms}$  (first peak time of B phase short current) under different short circuit conditions are shown in Fig. 8. It can be seen from the results that the electromagnetic force in conductors where short circuit fault happened is larger than other conductors. The distributions of electromagnetic force are influenced by the short circuit fault types and conductor space arrangement of GIB. During single B short circuit fault, the x-direction force component of B phase conductor is very small and the conductor vibration mainly along the vertical y-direction, the direction of short circuit electromagnetic force and vibration of tank are opposite to the conductor. During BC short circuit fault the short circuit electromagnetic forces are mainly distributed in the BC phase conductor and the tank short circuit electromagnetic force appears on the right half part which direction to BC phase conductors. During three-phase short circuit fault the short circuit electromagnetic force distributions of the conductor are the same as the

steady state condition which depend on the instantaneous values of short currents, and the short circuit electromagnetic force of tank rightly direct to the three phase conductors. Therefore 3 acceleration sensors

which are arranged on the tank of three phase conductors direction can be used for short circuit location of three phase enclosure GIB according to our analysis.

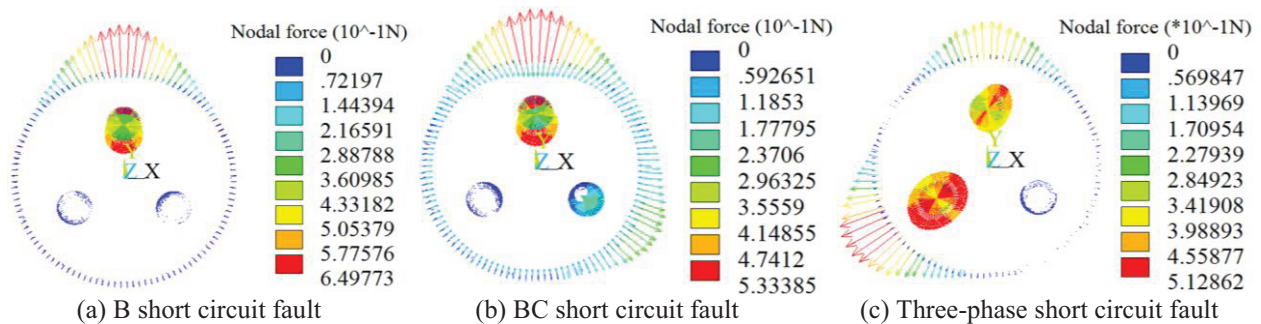


Fig. 8. Electromagnetic force of conductors and tank under different short circuit conditions at  $t=6.7ms$ .

**B. Distributions of short circuit electromagnetic force of plug-in connector**

The electromagnetic force distributions of contact fingers at  $t=6.7ms$  (peak time of B phase short current) under different short circuit conditions are shown in Fig. 9. Electromagnetic forces of A phase contact fingers and C phase contact fingers are influenced by the B phase conductor where short circuit current flows and the force amplitudes are rather small during single B phase short circuit fault, and the electromagnetic forces of B phase contact fingers are mainly influenced by the contact finger current distributions which are caused by conductor gravity. During BC short circuit fault the electromagnetic forces of B phase contact fingers and C phase contact fingers are strongly interacted with each other, whereas the conductor gravities have little influence on electromagnetic force distributions and the force amplitudes of B phase contact fingers are smaller than those of single phase short circuit fault. During three-phase short circuit fault the distributions of electromagnetic forces in different contact fingers are influenced by the instantaneous values of short currents which strongly interact with each other, and the force amplitudes of B contact fingers are smaller than those of single phase and BC short faults; the conductor gravities also have little influence on electromagnetic force distributions as BC short condition. Electromagnetic forces in contact fingers can reduce the contact force which is exerted by the holding springs and cause the transient contact degradation as mentioned in our previous work [18]. From analysis results in this work, it can be seen that the distributions of electromagnetic force in individual contact finger are influenced by the short circuit conditions, and some contact fingers with smaller contact forces may be seriously ablated by large short currents.

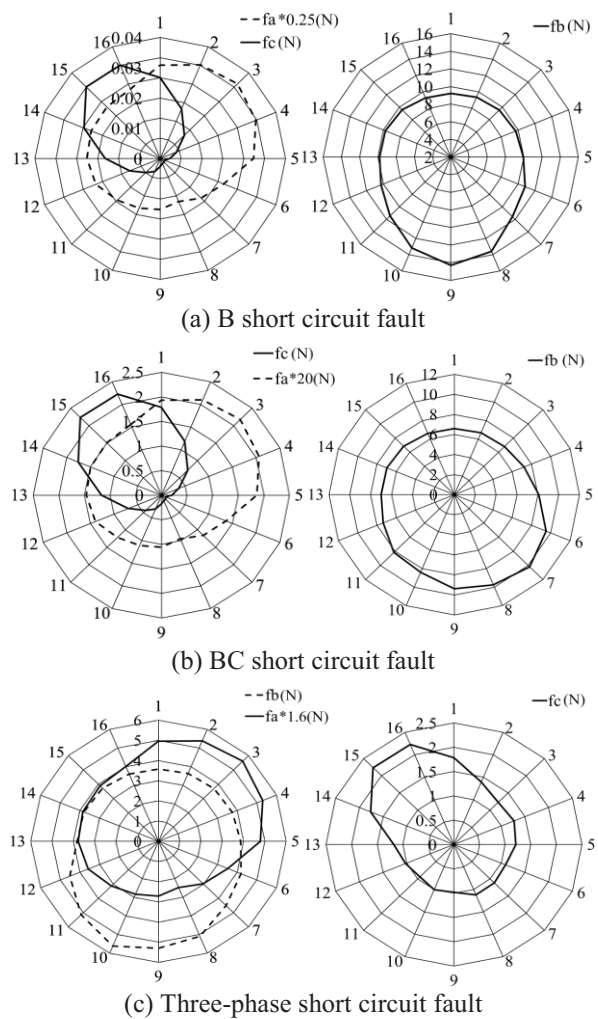


Fig. 9. Electromagnetic forces of plug-in connectors under different short circuit conditions at  $time=6.7ms$ .

**C. Transient short circuit electromagnetic forces characters of conductor and tank**

The transient electromagnetic force characteristics of B phase conductor and tank under different short circuit fault conditions are shown in Fig. 10 - Fig. 12. Transient short circuit electromagnetic forces of conductor and tank present space asymmetric vibration characteristics with fault time. Electromagnetic force amplitudes of B phase conductor and tank under single B phase short circuit fault are larger than those of two phase and three-phase short circuit faults according with the results described in [5]. The peak electromagnetic force moments under different short circuit conditions are not the same, and the moments of single B phase short circuit fault are earlier than those of BC short circuit and three short circuit faults.

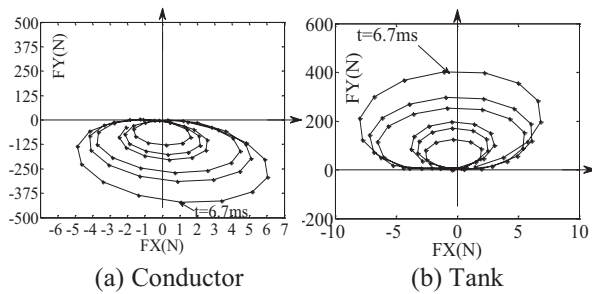


Fig. 10. Transient electromagnetic forces of B phase conductor and tank under B short circuit fault.

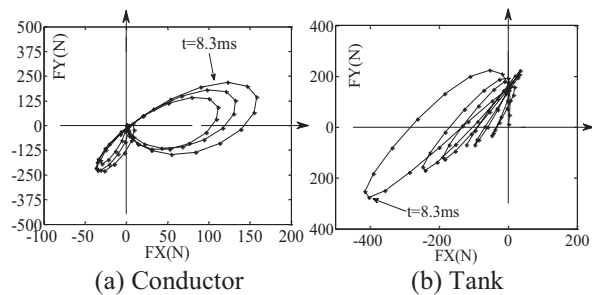


Fig. 11. Transient electromagnetic forces of B phase conductor and tank under BC short circuit fault.

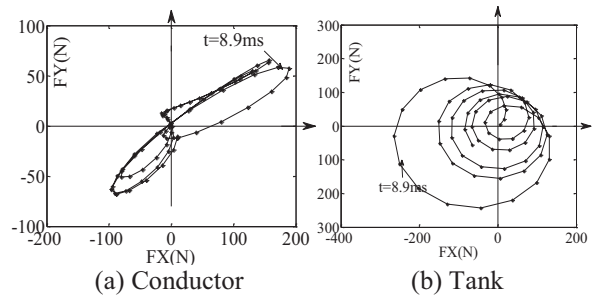


Fig. 12. Transient electromagnetic forces of B phase conductor and tank under three-short circuit fault.

The contact stability of three phase enclosure GIB capsule in which the conductors are supported only by two end plug-in connectors under short conditions must be taken into account seriously for the reason that large conductor electromagnetic forces (nearly 400N) together with repulsive forces between contact fingers will directly act on the plug-in connectors, which could cause serious contact degradation, even some contact fingers will lose contact and the whole connector may be damaged. Reliable contact finger positioning design which can withstand the short circuit impact is very important.

**VIII. CONCLUSION**

The current distribution and electromagnetic force calculation are essential for analyzing the contact degradation mechanism and the short circuit withstand capability of three phase enclosure type GIB capsule. Taking into account the distributions of contact force and the current constriction effect on the plug-in connectors, a 3-D circuit-field coupling FEM model has been developed for analyzing the dynamic current distributions and electromagnetic forces behaviors of three phase enclosure type GIB under steady state and different short circuit conditions. The validity of calculation model is demonstrated by vibration experiments and the following findings can be derived from this study.

The current distributions in the conductors and tank are not uniform because of skin effect and proximity effect. The current distributions in plug-in connectors are strongly influenced by the interactions between different phase conductor currents. Uneven temperature rise will be induced by the current distributions and some contact fingers can be overheating, leading to contact degradation.

The electromagnetic force and mechanical vibration of three phase enclosure GIB are relative small under steady state. However relatively large electromagnetic force can be exerted on them due to sharp increase of short circuit current and the distributions of electromagnetic force are directly influenced by the current distributions and conductor gravity. Electromagnetic force of individual contact finger is influenced by the short circuit conditions, contact forces of some contact fingers may decrease, even lost by the action of repulsive force and conductor electromagnetic force, some contact fingers with smaller contact force may be seriously ablated by large short currents. Electromagnetic forces of conductor and tank under single phase short circuit fault are larger than those of two phase and three-phase short circuit faults and the peak electromagnetic moments under different fault conditions are not the same. The results obtained by field-circuit coupling analysis can be used to optimal design and online monitoring of three phase

enclosure type GIB.

### ACKNOWLEDGEMENT

This work was supported by the Fundamental Research Funds for the China Central Universities (2012207020208).

### REFERENCES

- [1] A. H. Cookson and C. S. Cleale, "Three-conductor compressed gas cable optimization," *EPRI Project 7840 Final Report*, Feb. 1979.
- [2] Y. Mukaiyama, I. Takagi, K. Izumi, T. Sekiguch, A. Kobayashi, and T. Sumikawa. "Investigation on abnormal phenomena of contacts using disconnecting switch and detachable bus in 300kV GIS," *IEEE Trans. Power Delivery*, vol. 5, no. 1, pp. 189-195, 1990.
- [3] A. E. Emanuel, H. C. Doeppen, and P. C. Bolin, "Design and test of a sliding plug-in conductor connector for compressed gas-insulated cables," *IEEE Trans. Power Apparatus and Systems*, vol. 95, no. 2, pp. 570-579, 1976.
- [4] A. G. Kladas, M. P. Papadopoulos, and J. A. Tegopoulos, "Leakage flux and force calculation on power transformer windings under short-circuit: 2D and 3D models based on the theory of images and the finite element method compared to measurements," *IEEE Trans. Magnetics*, vol. 36, no. 4, pp. 3487-3490, 1994.
- [5] H. Hama, T. Marutani, K. Takatsuka, T. Nitta, and T. Tanabe, "Characteristics of short circuit electromagnetic forces in three phase enclosure type gas insulated bus," *IEEE Trans. Power Delivery*, vol. PWRD-2, no. 2, pp. 367-373, 1987.
- [6] S. Tominaga, H. Mukae, S. Matsuda, N. Okutsu, and Y. Takahashi, "Dynamic behavior of metal enclosures for gas insulated substations during ground faults and their immediate location by mechanical means," *IEEE Trans. Power Apparatus and Systems*, vol. PAS-98, no. 4, pp. 1283-1290, 1979.
- [7] Y. Kanno, T. Amemiya, N. Takahashi, and N. Kobayahi, "The short circuit electromagnetic force of the three-phase encapsulated gas insulated busbar," *IEEE Trans. Power Apparatus and Systems*, vol. PAS-103, no. 6, pp. 1386-1393, 1984.
- [8] H-K. Kim, J-K. Jung, K-Y. Park, C-H. Im, and H-K. Jung, "Efficient technique for 3-D finite element analysis of skin effect in current-carrying conductors," *IEEE Trans. Magnetics*, vol. 40, no. 2, pp. 1326-1329, 2004.
- [9] T. Takeuchi, T. Yoshizawa, and Y. Kuse, "3-D nonlinear transient electromagnetic analysis of short circuit electromagnetic forces in a three-phase enclosure-type gas insulated bus," *IEEE Trans. Magnetics*, vol. 36, no. 4, pp. 1754-1757, 2000.
- [10] D. Labirdis and V. Hatzianthassiou, "Finite element computation of field, forces and inductances in underground SF6 insulated cables using a coupled magneto-thermal formulation," *IEEE Trans. Magnetics*, vol. 30, no. 4, pp. 1407-1415, 1994.
- [11] S. Ito, Y. Takato, Y. Kawase, and T. Ota, "Numerical analysis of electromagnetic forces in low voltage ac circuit breakers using 3-D finite element method taking into account eddy currents," *IEEE Trans. Magnetics*, vol. 34, no. 5, pp. 2597-2600, 1998.
- [12] K. Yoshihiro, M. Hiroyuki, and I. Shokichi, "3-D finite element analysis of electro-dynamic repulsion forces in stationary electric contacts taking into account asymmetric shape," *IEEE Trans. Magnetics*, vol. 33, no. 2, pp. 1994-1999, 1997.
- [13] G. Bedrosian, "A new method for coupling finite element field solutions with external circuits and kinematics," *IEEE Trans. Magnetics*, vol. 29, no. 2, pp. 1664-1668, 1993.
- [14] M. R. Shah, G. Bedrosian, and J. Joseph, "Steady-state loss and short-circuit force analysis of a three-phase bus using a coupled finite element + circuit approach," *IEEE Trans. Energy Conversion*, vol. 14, no. 4, pp. 1485-1489, 1999.
- [15] J. Weiss and V. K. Jarg, "Steady state eddy current analysis in multiply-excited magnetic systems with arbitrary terminal conditions," *IEEE Trans. Magnetics*, vol. 24, no. 6, pp. 2676-2678, 1988.
- [16] G. B. Kumbhar and S. V. Kulkarni, "Analysis of short-circuit performance of split-winding transformer using coupled field-circuit approach," *IEEE Trans. Power Delivery*, vol. 22, no. 2, pp. 936-943, 2007.
- [17] M. van der Giet, E. Lange, D. A. P. Corrêa, I. E. Chabu, S. I. Nabeta, and K. Hameyer, "Acoustic simulation of a special switched reluctance drive by means of field-circuit coupling and multi-physics simulation," *IEEE Trans. Industrial Electronics*, vol. 57, no. 9, pp. 2946-2953, 2010.
- [18] X. Guan and N. Shu, "Electromagnetic field and force analysis of three-phase enclosure type GIS bus capsule," *Applied Computational Electromagnetics Society Journal*, vol. 29, no. 8, pp. 582-589, 2014.
- [19] R. Holm, *Electric Contacts: Theory and Applications*, Springer, New York, 1979.



**Xiangyu Guan** received the B.S. degree in Environmental Science from Xinjiang Normal University, China, in 2010 and the M.S. degree in Power Electronics from Wuhan University, Hubei, China, in 2012. He is a Ph.D. candidate in Electrical Engineering College Wuhan University. He is Members of ACES and ICS, his research interests mainly focus on numerical methods of field calculation and condition monitoring of electrical equipment.

**Bing Kang** received the B.S. degree in Electrical Engineering from Beijing Institute of Petrochemical Technology, China, in 2010 and the M.S. degree in Electrical Engineering from Wuhan University, Hubei, China, in 2012. He is currently a Ph.D. candidate in School of Electrical Engineering Wuhan University. His research interest includes transient overvoltage and electromagnetic transient in power system.

**Naiqiu Shu** is a Professor in Electrical Engineering College Wuhan University. He received his M.S. and Ph.D. degrees in Electrical Engineering College Wuhan University. His research interests mainly focus on sensor technology and condition monitoring of electrical equipment.

**Qiangqiang Yan** received the B.E. degree in Electrical Engineering and Automation from China University of Mining and Technology, in 2013. He is now currently pursuing his M.S. degree in Electrical Engineering and its Automation from Wuhan University, Hubei, China. His primary research interests include numerical methods of field calculation and condition monitoring of electrical equipment.

**Zipin Li** is an Associate Professor in Electrical Engineering College Wuhan University. He received his M.S. and Ph.D. degrees in Electrical Engineering College Wuhan University. His research interests mainly focus on condition monitoring of electrical equipment.